Printed in U.S.A.

78-GT-136

an ASME publication

$3.00 PER COPY
$1.50 TO ASME MEMBERS
1.00 £ at Wembley

Erosion Study in Turbomachinery Affected by Coal Ash Particles

W. TABAKOFF

Professor
Mem. ASME

R. KOTWAL

Graduate Research Assistant

A. HAMED

Associate Professor
Mem. ASME

University of Cincinnati,
Cincinnati, Ohio

Turbomachinery operating with coal particles or using pulverized coal as fuel are exposed to erosion. The problem of predicting erosion in rotating machinery is very complex. The present paper describes the test facility which is designed in such a way that the aerodynamic effects are an integral part of the erosion test parameters. Some results from the alloys studied (aluminum, stainless steel, and titanium) in this investigation are reported.

Contributed by the Gas Turbine Division of The American Society of Mechanical Engineers for presentation at the Gas Turbine Conference & Products Show, London, England, April 9-13, 1978. Manuscript received at ASME Headquarters December 22, 1977.

Copies will be available until January 1, 1979.

THE AMERICAN SOCIETY OF MECHANICAL ENGINEERS, UNITED ENGINEERING CENTER, 345 EAST 47th STREET, NEW YORK, N.Y. 10017

Erosion Study in Turbomachinery Affected by Coal Ash Particles

W. TABAKOFF **R. KOTWAL** **A. HAMED**

NOMENCLATURE

D = particle diameter
K_1, K_{12}, K_3 = material constants
V = particle velocity
β = relative angle between particle path and specimen surface
ϵ = erosion per unit mass of impacting particles
μ = microns

Subscripts

1 = conditions of the particle approaching the target
2 = conditions of the particle rebounding from the target
N = normal component
T = tangential component

INTRODUCTION

The design and development of high performance turbomachinery (compressors and turbines) operating in an ambient with coal particles or coal ash requires a thorough knowledge of the fundamental phenomena upon which the future of advanced turbomachinery for use in the coal industry, gasification, mining, pipelines' gas transport, powder coal burning, coal-oil gas refinery, and many others is dependent. By coal gasification, a particulate flow is formed from coal and catalyst. Large particles are separated out by cyclones, but a quantity of particles from 5 to 25 microns pass through the cyclones and enter the turbine. With these particles, the life of the turbine is very limited.

In the present and in the future, the use of pulverized coal as fuel in many power plants and industrial establishments is inevitable. Burning coal and the products of combustion will contain solid particles. Presence of such solid particles through the combustor and the converting energy device will produce erosion to the engine components and in a very short time possible deterioration of engine power output.

Erosion has been pointed out as a problem in as diverse areas as aero gas turbine, transport tube, coal-fired boiler systems, and catalytic cracking equipment. Air filtration has been used for fixes of this problem; however, filtration cannot be accomplished 100 percent, and it reduces the engine performance. The problem of predicting erosion in rotating machinery is very complex and has not been satisfactorily discussed in the literature. This complexity is primarily a result of the fact that the particle trajectory must be traced through the flow field after multiple impacts. If erosion could be incorporated as an engine design parameter, perhaps an erosion tolerant engine could be produced.

Historically, erosion has been studied as a two-part problem. The first part involves the determination of the number, direction, and velocity of the particles striking the surface which is naturally affected by the flow conditions. With such information available, the second part of the problem involves the calculation of the surface material removed. These two problems have always been considered to be independent of one another; however, in the complicated flow fields existing within rotating machinery, it is questionable whether this assumption is valid.

The theoretical studies concerning erosion are predominantly empirical. They involve basic assumptions as to the process governing material removal. Finnie (1)[1] and Smeltzer, et al. (2) have conducted theoretical analyses of the erosion of ductile materials. In more recent investigations (3-5), further insight into the actual mechanism of erosion has been obtained by examining the target surface at high magnification using metallographic techniques and electron microscopy. Fraas (3) summarizes the principal

[1] Numbers in parentheses designate References at end of paper.

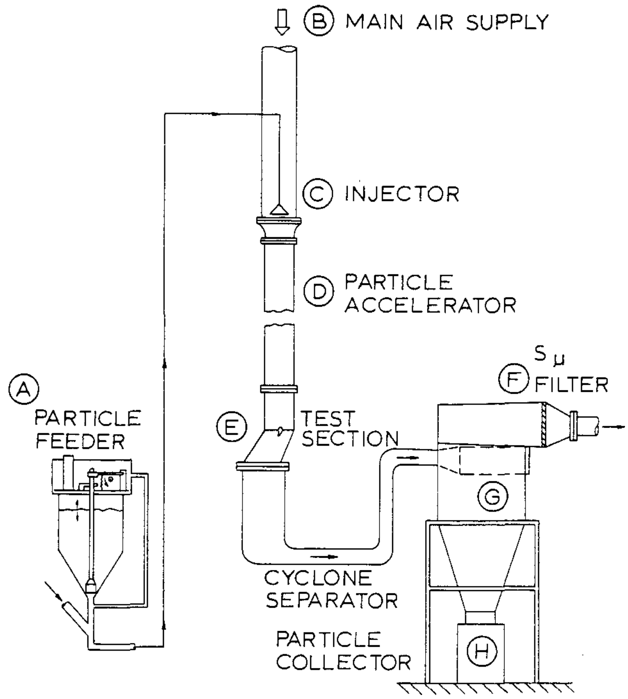

Fig. 1 Erosion test schematic. Erosion research facility

information obtained from a comprehensive survey of turbine bucket erosion.

In 1959, Finnie (4) described a sand-blasting erosion test facility. This facility incorporated a small jet of particle-laden air impacting on a stationary specimen. By far the majority of erosion research has been conducted using this facility or modifications of it.

EXPERIMENTAL EQUIPMENT

As mentioned previously, the test facilities designed thus far did not simulate the aerodynamic effect of the flow field over the erosion specimen. This effect can be a very important factor in turbomachine erosion, where the flow is constantly turned by rotating and stationary cascades. Two erosion test facilities were, therefore, built during the course of this study. The first wind tunnel with a stationary specimen was designed to obtain basic erosion data, particle impact, and rebound characteristics. Another unique test facility was then designed to simulate and measure the erosion of turbomachine blades.

Stationary Specimen Test Facility

In designing this wind tunnel, controlling the various erosion parameters — such as fluid velocity, particle velocity, particle flow rate, and particle size — was of primary importance. The effects of variations in the specimen size, as well as the angle of incidence between the abrasive particles and the surface of the specimen, were also investigated. Besides obtaining erosion data in an aerodynamic environment, this test facility was also used to determine the particle impact and rebound characteristics using high-speed photography.

Fig. 1 is a schematic of the apparatus developed for that purpose. As depicted in this illustration, the equipment functions as follows: a measured amount of abrasive grit of a given consistency is placed into the particle feeder, A. The particles are fed into a secondary air source and blown up to the particle injector, C, where it mixes with the main air supply, B. The particles are then accelerated by the high velocity air in a constant area duct, D, and impact the specimen in test section, E. The test dust is then separated from the air by a cyclone separator, G, and collected in the container, H. The test air is further filtered through a commercial 5μ filter, F.

Since the particles are accelerated in the constant area duct by the aerodynamic drag forces, their velocity before impacting the specimen would depend upon the air velocity, the particle size, and the length of the acceleration section, D. Fig. 2 gives an illustration of the dynamics of relatively large, 200μ, and relatively small, 20μ, particles in two flow velocity fields, 122 and 305 m/s. From this figure, it can be seen that the particle's final velocity is an exponential function of the tunnel length.

From Fig. 1, it can be seen that the tunnel geometry is uninterrupted from the acceleration tunnel into the test section. In this manner, the particle-laden air is channeled over the specimen and the aerodynamics of the fluid passing over the blade at the given angle of attack are preserved. In order to minimize the tunnel blockage, three sized specimens were used. At angles of attack of 0 to 20 deg, a 25.4-mm-wide specimen was used; from 20 to 45 deg, a 12.7-mm wide specimen was used; and for the large angles of attack of 45 to 90 deg, a 6.35-mm-wide specimen was used.

The test section has an insert through which high-speed photography and streak photographs can be taken of the high-speed sand particles. In this manner, the velocity of the approaching sand particle was obtained and compared to the theoretical predictions.

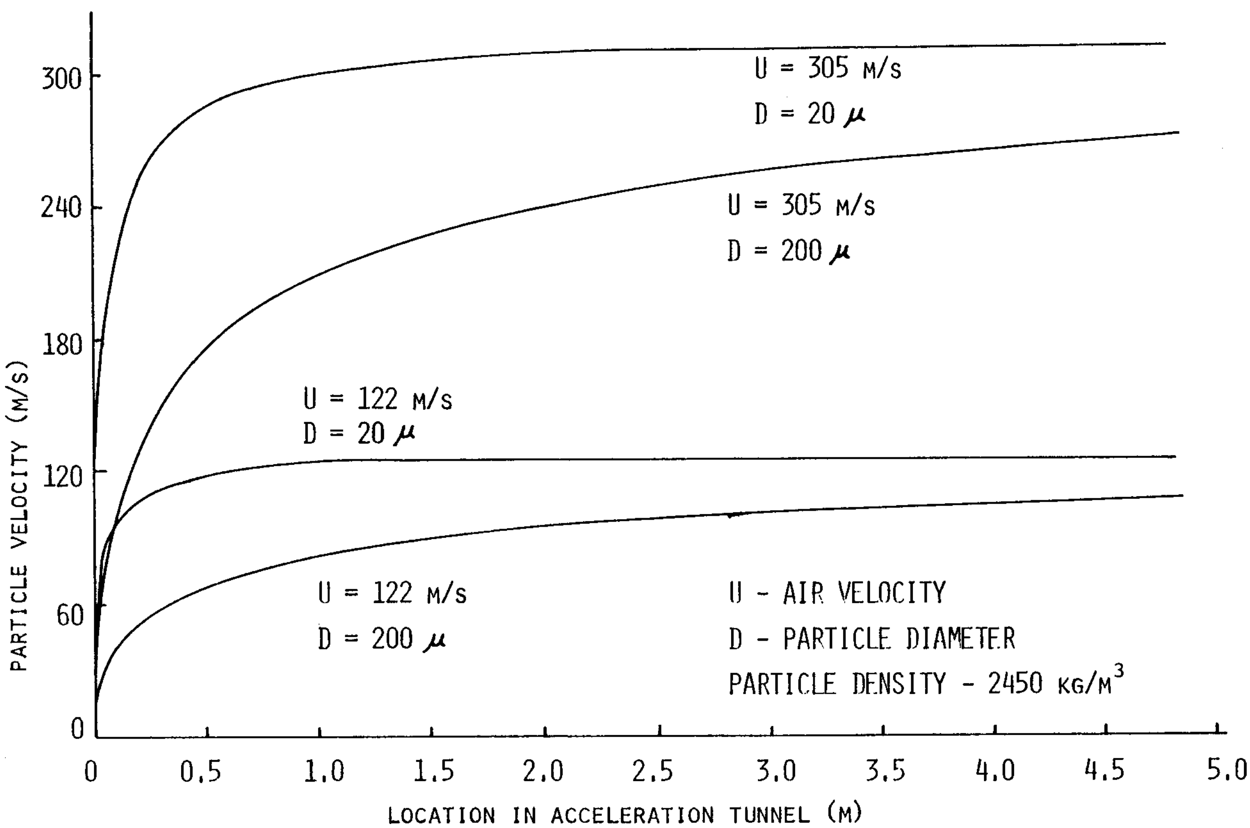

Fig. 2 Particle dynamics in a constant area acceleration tube

DEVELOPMENT OF PARTICLE REBOUND CORRELATIONS

The erosion of metals impacted by small dust particles, as well as the rebound dynamics of these particles, can only be described in a statistical sense. This becomes obvious when one examines the number of geometric situations that might be involved at impact. After a given incubation period, the target material will become pitted with craters and, in fact, after a slightly longer period, a regular ripple pattern may form on the eroded surface. Thus, the local impact angle between the small particle and the eroded surface may deviate considerably from the geometric average. Further, the particles themselves are irregular crystalline in shape with several sharp corners. Therefore, as the particle approaches the specimen, the orientation of the particle is, for the most part, random.

The restitution coefficient or restitution ratio is a measure of the kinetic energy exchange between two objects upon impact. Since erosion is a function of the energy exchange between the erodent particle and the material impacted, it was felt that the restitution ratio will give a good indication of the behavior of the particle-material interaction. This investigation was limited to ductile target materials only. In addition, the contaminant particles were chosen to be much harder than the target material. Therefore, the restitution ratio will be a measure of target distortion rather than distortion of the erosive particle.

Grant, Ball, and Tabakoff (5) were the first to thoroughly investigate the rebound characteristics of high-speed eroding particles. The study was carried out on annealed 2024 aluminum alloy. The data was described using histograms to illustrate its statistical distribution. It was concluded from this investigation that the restitution ratio (V_2/V_1), which is directly related to the kinetic energy lost during impact, does not give sufficient information in regard to erosion. With this in mind, the restitution ratio was broken down into a normal velocity restitution ratio, V_{N_2}/V_{N_1} (the normal component of the particle velocity after impact/the normal component of the particle velocity before impact), and a tangential velocity restitution ratio, V_{T_2}/V_{T_1} (the tangential component of the particle velocity after impact/the tangential component of the particle velocity before impact). It was

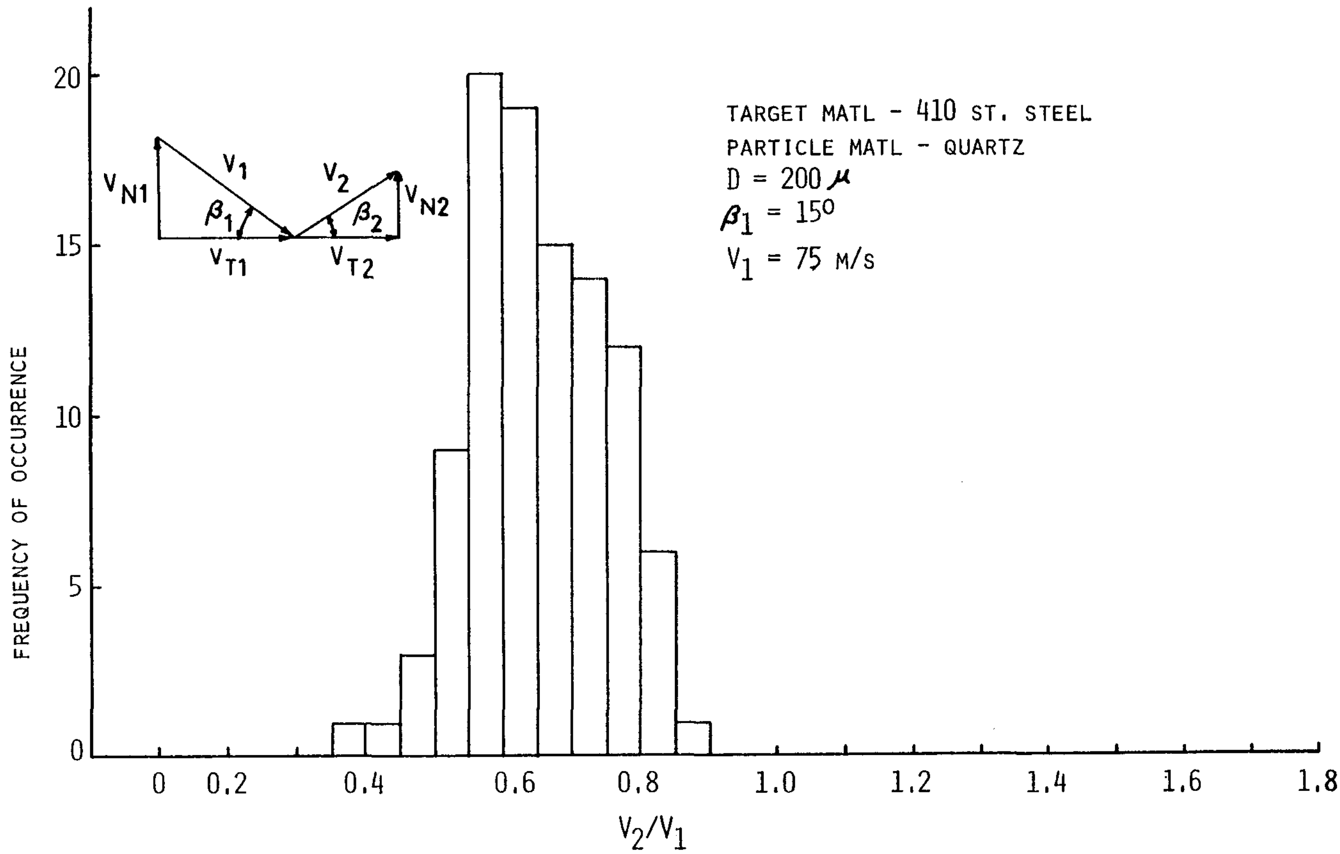

Fig. 3 Erosive particle velocity restitution ratio distribution

Table 1

Property \ Material	2024 Aluminum	6Al-4V Titanium	AISI 304 Stainless Steel	AISI 410 Stainless Steel
Composition	4.2 Cu, 0.5 Mn, 1.4 Mn, 0.5 Si, 0.5 Fe, 0.25 Zn, 0.1 Cr, Rest Al.	6.0 Al, 4.0 V, 0.08 C, 0.05 N, 0.2 O, 0.25 Fe, Rest Ti.	0.08 C, 2.0 Mn, 1.0 Si, 19.0 Cr, 10.0 Ni, Rest Fe.	0.15 C, 1.0 Mn, 1.0 Si, 0.04 P, 0.03 S, 12.0 Cr, Rest Fe.
Density lb/in^3	0.1	0.16	0.29	0.28
Melting temp. °F	935-1180	2920-3020	2550-2650	2700-2790
Mod. of elasticity (psi)	10.6×10^6	16×10^6	28×10^6	29×10^6
Thermal conductivity Btu/hr-ft °F	120	4.0	10.0	15.0
Tensile strength (psi)	27,000	130,000	75,000	65,000
Rockwell hardness		C30	B80	B80

found that the normal velocity restitution ratio does not significantly contribute to ductile erosion. Most probably the kinetic energy is dissipated by plastic deformation of the target material without significant material removal.

Fig. 3 illustrates the histogram of the

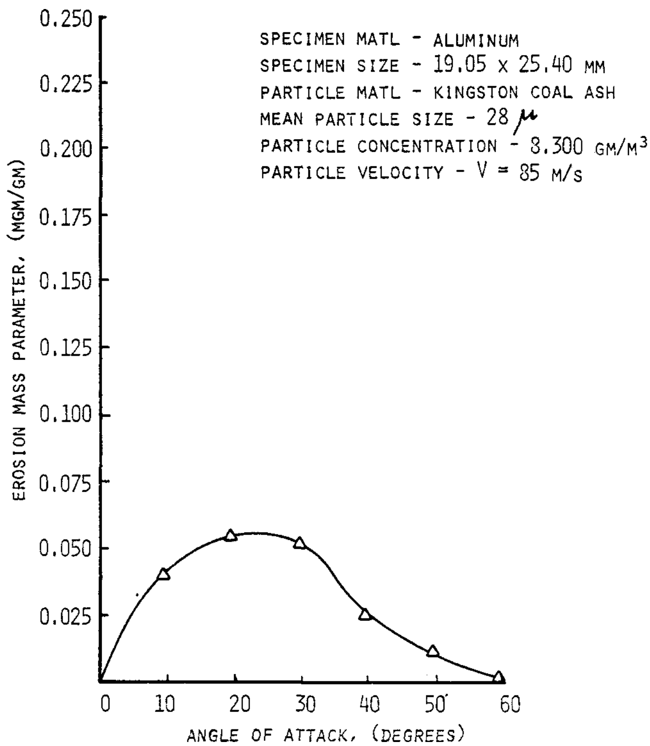

Fig. 4 Influence of particle impact angle on erosion of 2024 aluminum alloy (experimental results)

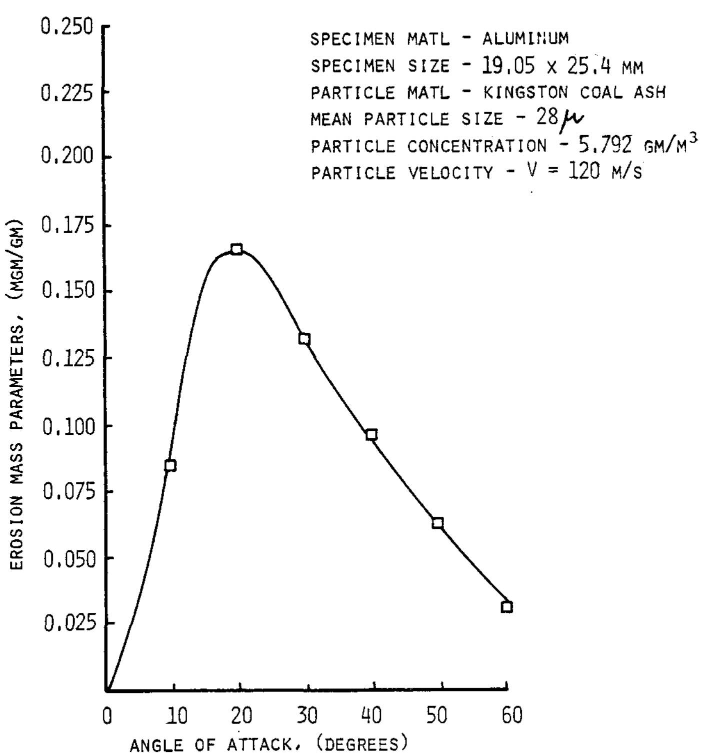

Fig. 5 Influence of particle impact angle on erosion of 2024 aluminum alloy (experimental results)

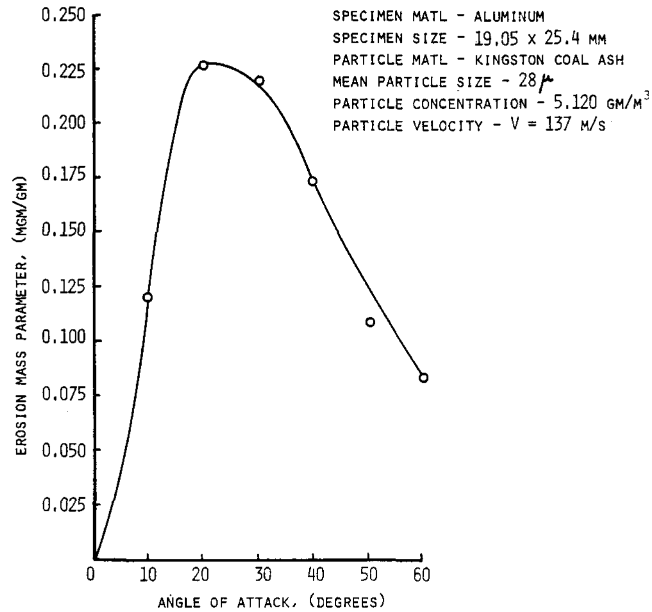

Fig. 6 Influence of particle impact angle on erosion of 2024 aluminum alloy (experimental results)

velocity restitution ratio for stainless steel at an angle of attack of 15 deg. As can be seen from this figure, the data is presented by a series of rectangles. The height of the rectangle represents the number of times or frequency of occurrence that the velocity restitution ratio was found to be between the limits designated by the scale at the base of the rectangle. The spread in the data indicates that the condition of the material surface and the orientation of the particle at impact changes.

EXPERIMENTAL RESULTS

The previously described erosion test facility was used to obtain the basic erosion data. The material erosion in this study was determined by measuring the weight of the specimen before and after the testing. The target materials used were 2024 aluminum 6Al-4V titanium and 304 stainless steel. The properties of these materials are given in Table 1. The abrasive particles used consisted of West Virginia coal ash. In this investigation, the parameters which influence the extent of the erosion damage such as angle of attack and particle velocity received close attention. In all tests, the specimen size was 19.0 x 25.4 mm. The experiments were performed with Kingston coal ash with mean particle size of 28 microns and the particle velocities of 85, 120, and 137 m/s.

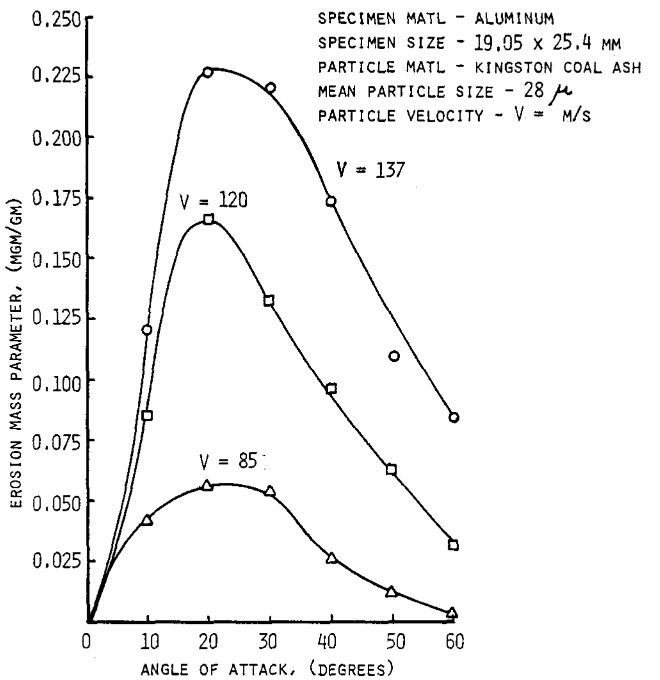

Fig. 7 Influence of particle impact angle on erosion of 2024 aluminum alloy (experimental results)

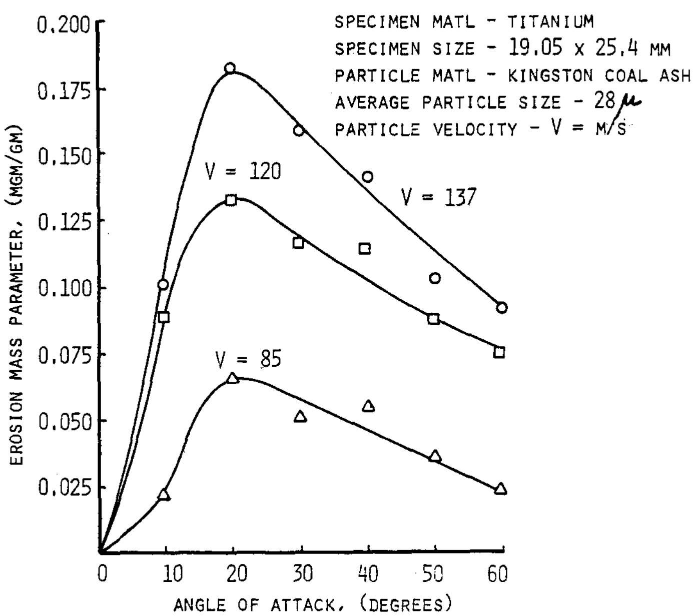

Fig. 8 Influence of particle impact angle on erosion of 6Al-4V titanium alloy (experimental results)

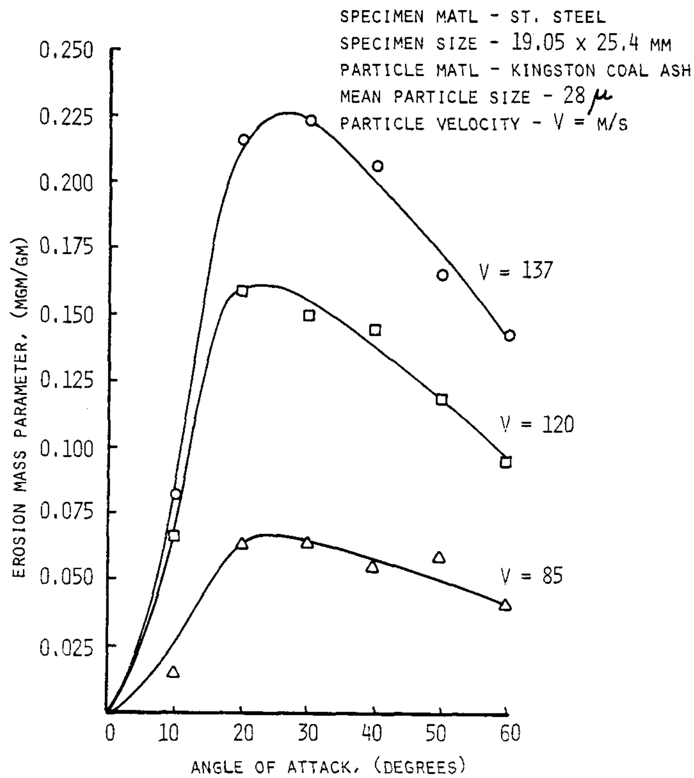

Fig. 9 Influence of particle impact angle on erosion of 304 stainless steel (experimental results)

Effect of Angle of Attack and Particle Velocity

One of the important parameters that affect materials erosion is the angle of attack at which particles strike the target surface. Figs. 4, 5, and 6 illustrate test results for the influence of the angle of attack on the erosion of aluminum alloys at three different particle velocities. From these figures, it can be seen that for all the velocities tested, the erosion mass parameter (expressed as milligram of material eroded per gram of abrasive impacted on the specimen surface), has a maximum value at an angle of attack of approximately 20 deg. The test results for the three velocities are combined together in Fig. 7, which shows how the material removal rate is influenced by this angle. From the inspection of the figure, it may be seen that as the angle of attack increases over 20 deg, the erosion reduces to a residual value at 90 deg. The effect of the angle of attack is independent of the particle velocities; however, the definition of the point of maximum erosion becomes much more explicit with increasing velocity. During all the tests conducted, the tunnel was free from blockage, so that erosion could be measured without destroying the aerodynamic environment. Special attention was given to the specimen surface finishes.

The effects of impingement angle and particle velocity on erosion of 6Al-4V titanium are shown in Fig. 8. The test conditions were identical to that of the previous case. For titanium

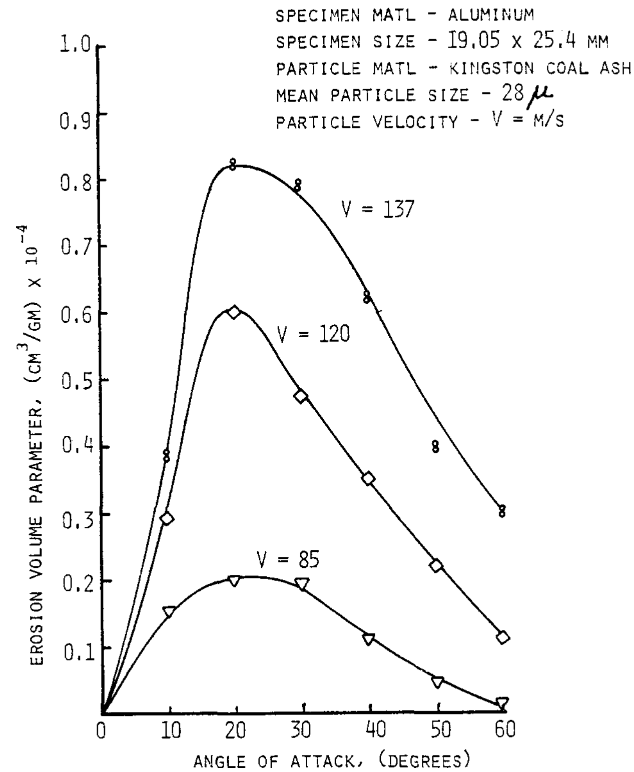

Fig. 10 Values of experimental erosion volume parameter for 2024 aluminum alloy

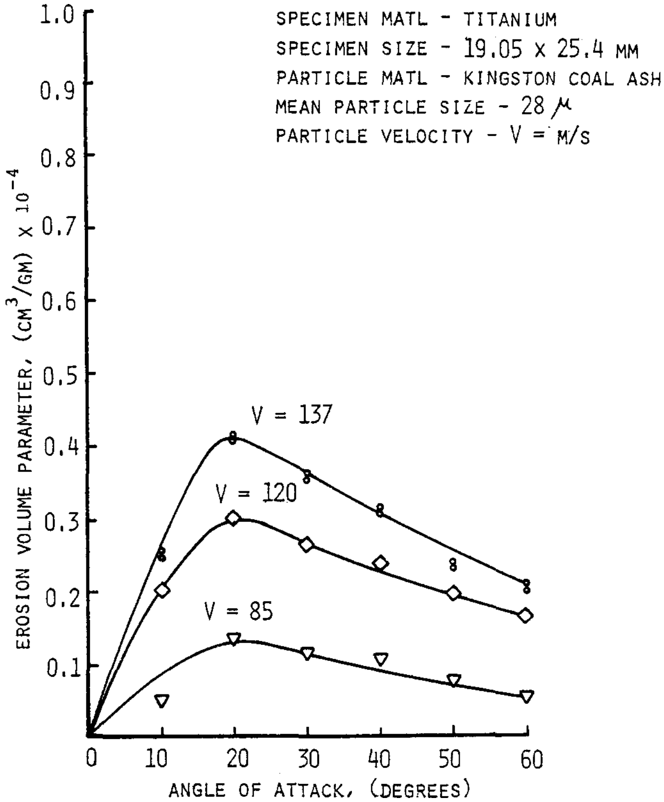

Fig. 11 Values of experimental erosion volume parameter for 6Al-4V titanium alloy

alloy also, the maximum erosion occurred approximately at an angle of 20 deg. It can be seen from Figs. 7 and 8 that the general trend of the erosion curves for 6Al-4V titanium is similar to that of aluminum.

The erosive characteristics of another target material, namely 304 stainless steel is shown in Fig. 9. For this material, the angle at which maximum erosion occurs is approximately 25 deg. To compare the erosion of these different target materials having different densities, they were expressed in terms of erosion volume parameter. It is expressed as the volumetric material loss caused by unit weight of ash impacted on the specimen surface. These results are presented in Figs. 10, 11, and 12. It can be seen that for all angles of impact at three different velocities tested, the volumetric erosion of stainless steel and aluminum differ by almost three orders of magnitude and that of titanium and aluminum by about two orders of magnitude. To study the influence of the nature of particles on the erosion of different target materials, the present results with coal ash particles were compared with the results obtained by Ball and Tabakoff (6) for quartz and alumina particles. The results of this comparison are shown in Figs. 13, 14, and 15.

It can be seen that, by an impingement angle of 20 deg, the erosiveness of alumina and quartz particles are about 70 and 40 percent greater than that of coal ash at the same conditions. From the physical analysis of the coal ash used, Tabel 2 shows that it contains 55 percent of SiO_2, 30 percent of Al_2O_3, and other compounds. The erosion mass parameters in the last three figures are very consistent in regard to particle materials and particle sizes. If the average size of the coal ash particles were about 110μ, the erosion damage would be greater than that caused by the quartz particles. However, it is observed that the erosion damage caused by coal ash particles is much lower due to their smaller size as compared to erosion damage caused by alumina and quartz particles. The results of the tests conducted also show that the angle of maximum erosion is dependent not only on the target material, but also on the type of the particle material.

PREDICTION OF EROSION FOR DIFFERENT MATERIALS

The following equation was developed by Grant and Tabakoff (7) to predict the erosion of

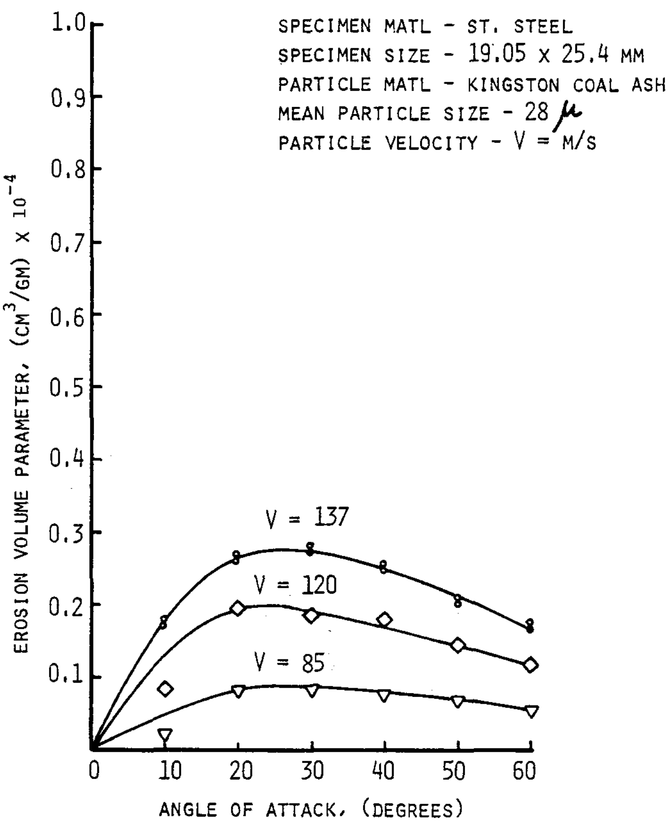

Fig. 12 Values of experimental erosion volume parameter for 304 stainless steel

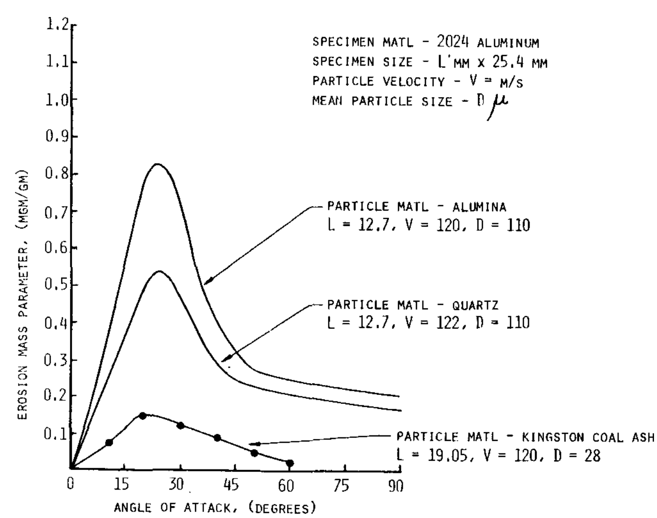

Fig. 13 The effect of particle material on erosion of aluminum alloy

ductile alloys:

$$\epsilon = K_1\, f(\beta_1)\, V_1^2 \cos^2\beta_1 \left[1 - R_T^2\right] + f(V_{IN})$$

$$R_T = 1 - 0.0016\, V_1 \sin\beta_1$$

$$f(\beta_1) = \left[1 + CK\left\{K_{12} \sin\left(\frac{90}{\beta_o}\right) \beta_1\right\}\right]^2$$

$$f(V_{IN}) = K_3\, (V_1 \sin\beta_1)^4$$

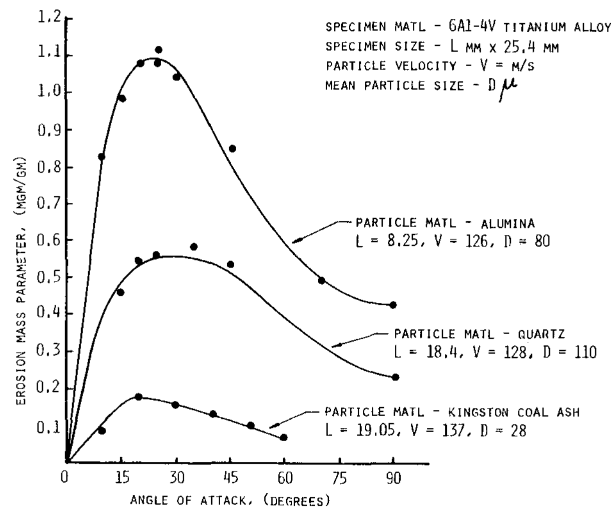

Fig. 14 The effect of particle material on erosion of titanium alloy

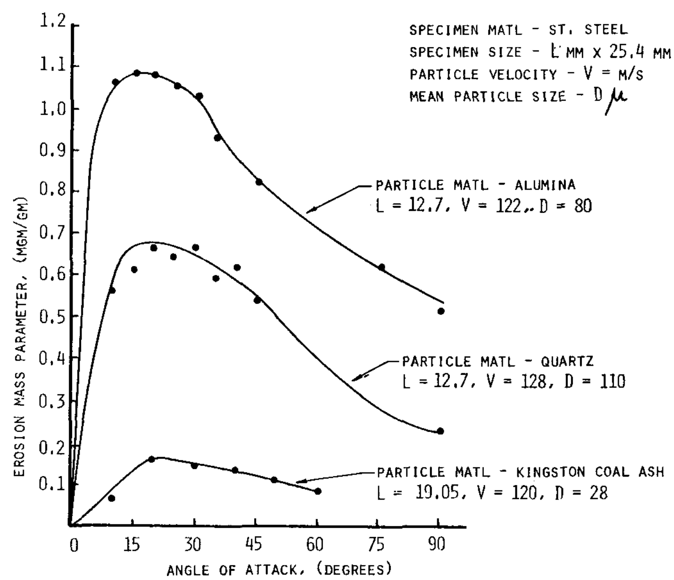

Fig. 15 The effect of particle material on erosion of stainless steel

where:

- ϵ = erosion per unit mass of impacting particles
- β_1 = relative angle between particle path and specimen surface
- β_o = angle of maximum erosion
- V_1 = particle velocity
- R_T = tangential restitution ratio
- CK = 1 for $\beta_1 \leq 3\beta_o$
- CK = 0 for $\beta_1 > 3\beta_o$.

The foregoing equation was developed assuming that the erosion process is characterized by two

Table 2 Ash Analysis of West Virginia Coal (Kingston)

Ash Analysis		
SiO_2	(%)	54.39
Al_2O_3	(%)	28.58
Fe_2O_3	(%)	10.08
$Ti\ O_2$	(%)	0.47
$Ca\ O$	(%)	1.28
$Mg\ O$	(%)	1.04
Na_2O	(%)	0.20
$K_2\ O$	(%)	2.09
SO_3	(%)	1.03
P_2O_5	(%)	0.06
Undetermined	(%)	0.78
		100.00
Heating value as rec'd (Btu/lb)		12,820

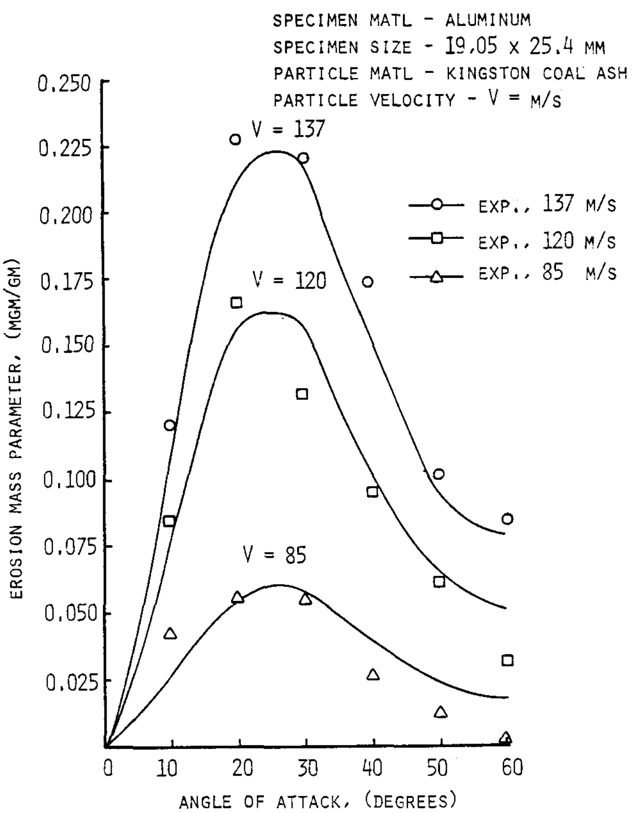

Fig. 16 Experimental and predicted erosion results for 2024 aluminum alloy

mechanisms at low and high impingement angles. The foregoing equations include the relationship for erosion damage at low angles of impingement, at high angles of impingement, and a combination of the two at intermediate approach angles.

The experimental data for ash impacting

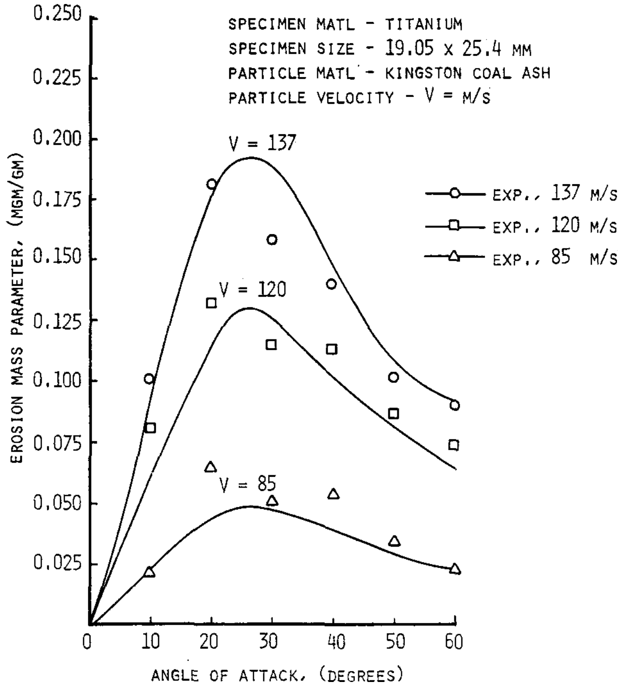

Fig. 17 Experimental and predicted erosion results for 6Al-4V titanium

the aluminum, titanium, and stainless-steel alloys were substituted into the Grant and Tabakoff (7) equation, and from the corresponding results, it was possible to determine the empirical constants, K_1, K_{12}, and K_3. This was accomplished numerically to obtain a least squares fit to a nonlinear function. The empirical constants for the different materials erosion by coal ash particles were found to be as follows: (a) for aluminum, $K_1 = 1.56988 \times 10^{-6}$, $K_{12} = 0.3193$, and $K_3 = 2.0 \times 10^{-12}$; (b) for titanium, $K_1 = 1.564951 \times 10^{-6}$, $K_{12} = 0.173636$, and $K_3 = 3.0 \times 10^{-12}$; (c) for stainless steel, $K_1 = 1.505101 \times 10^{-6}$, $K_{12} = 0.296077$, and $K_3 = 5.0 \times 10^{-12}$. These constants were used in the empirical equation and the computed erosion rates are compared to the experimental results in Figs. 16, 17, and 18. The predicted curves are found to fall generally within the experimental points, but the predicted angle of maximum erosion is slightly higher than the experimentally determined value.

The basic information developed and the empirical relations derived provide the necessary data for the material removed by erosion. This, together with an analysis of particle trajectories in turbomachines (8), can be used in the prediction of the different turbine components by the ash particles.

CONCLUSION

This study shows how the erosion damage in turbomachinery utilizing coal can be predicted.

ACKNOWLEDGMENT

This work was sponsored by ERDA Contract No. E(49-18)-2465.

REFERENCES

1 Finnie, I., Wolak, J., and Kabil, Y., "Erosion of Metals by Solid Particles," Journal of Materials, Vol. 2, No. 3, Sept. 1967, pp. 682-700.

2 Smeltzer, C. E., et al., "Mechanisms of Sand and Dust Erosion in Gas Turbine Engines," USAAVLABS Technical Report, Aug. 1970.

3 Fraas, A. P., "Survey of Turbine Bucket Erosion, Deposits, and Corrosion," ASME Paper No. 75-GT-123, presented at the Gas Turbine Conference, Houston, Texas, March 2-6, 1975.

4 Finnie, I., "An Experimental Study on Erosion," Proceedings of the Society for Experimental Stress Analysis, Vol. 17, No. 2, pp. 65-70.

5 Grant, G., Ball, R., and Tabakoff, W., "An Experimental Study of the Erosion Rebound Characteristics of High-Speed Particles Impacting a Stationary Specimen," Department of Aerospace Engineering Technical Report 73-36, May 1970 (AD-760578).

6 Ball, R., and Tabakoff, W., "An Experimental Investigation of the Erosive Characteristics of 410 Stainless Steel and 6Al-4V Titanium," Department of Aerospace Engineering Technical Report 73-40, University of Cincinnati, Ohio, July 1973 (AD-774325).

7 Grant, G., and Tabakoff, W., "An Experimental Investigation of the Erosive Characteristics of 2024 Aluminum Alloy," Department of Aerospace Engineering Technical Report 73-37, University of Cincinnati, Ohio, June 1973 (AD-764267).

8 Grant, G., and Tabakoff, W., "Erosion Prediction in Turbomachinery Resulting from Environmental Solid Particles," Journal of Aircraft, Vol. 12, No. 5, May 1975, pp. 471-478.

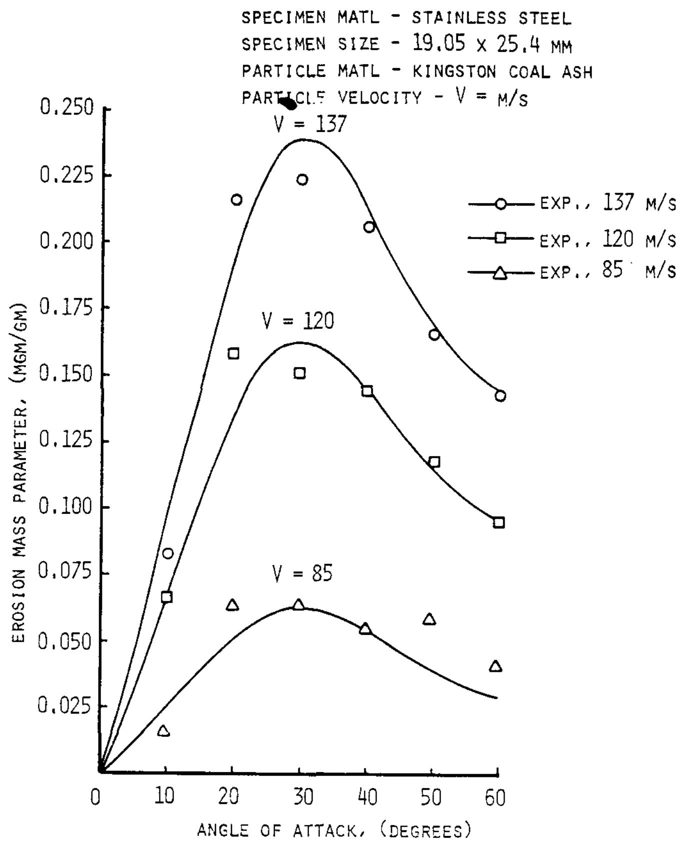

Fig. 18 Experimental and predicted erosion results for 304 stainless steel